
THE ITERATED GOLUB-KAHAN-TIKHONOV METHOD

A PREPRINT

Davide Bianchi

School of Mathematics (Zhuhai)
Sun Yat-sen University
Zhuhai 518055 (China)
bianchid@mail.sysu.edu.cn

Marco Donatelli

Dipartimento di Scienza e Alta Tecnologia
Università dell'Insubria
Como 22100 (Italy)
marco.donatelli@uninsubria.it

Davide Furchi

Dipartimento di Scienza e Alta Tecnologia
Università dell'Insubria
Como 22100 (Italy)
dfurchi@uninsubria.it

Lothar Reichel

Department of Mathematical Sciences
Kent State University
Kent OH 44242 (USA)
reichel@math.kent.edu

ABSTRACT

The Golub-Kahan-Tikhonov method is a popular solution technique for large linear discrete ill-posed problems. This method first applies partial Golub-Kahan bidiagonalization to reduce the size of the given problem and then uses Tikhonov regularization to compute a meaningful approximate solution of the reduced problem. It is well known that iterated variants of this method often yield approximate solutions of higher quality than the standard non-iterated method. Moreover, it produces more accurate computed solutions than the Arnoldi method when the matrix that defines the linear discrete ill-posed problem is far from symmetric.

This paper starts with an ill-posed operator equation in infinite-dimensional Hilbert space, discretizes the equation, and then applies the iterated Golub-Kahan-Tikhonov method to the solution of the latter problem. An error analysis that addresses all discretization and approximation errors is provided. Additionally, a new approach for choosing the regularization parameter is described. This solution scheme produces more accurate approximate solutions than the standard (non-iterated) Golub-Kahan-Tikhonov method and the iterated Arnoldi-Tikhonov method.

Keywords Large linear discrete ill-posed problem · Golub-Kahan-Tikhonov

1 Introduction

Let $T: \mathcal{X} \rightarrow \mathcal{Y}$ denote a bounded linear operator between separable Hilbert spaces \mathcal{X} and \mathcal{Y} with norms $\|\cdot\|_{\mathcal{X}}$ and $\|\cdot\|_{\mathcal{Y}}$, respectively, that are induced by inner products. We are concerned with operators T that are not continuously invertible. Such operators arise, for instance, from Fredholm integral equations of the first kind.

We consider the solution of linear operator equations of the form

$$Tx = y, \quad x \in \mathcal{X}, \quad y \in \mathcal{Y}, \quad (1)$$

which we assume to be solvable, and denote the unique least-squares solution of minimal norm by x^\dagger . Since T is not continuously invertible, x^\dagger might not depend continuously on y . The computation of the solution of (1) therefore is an *ill-posed problem*.

In many problems of the form (1) of interest in applications, the right-hand side is not known. Instead, only an error-contaminated approximation $y^\delta \in \mathcal{Y}$ of y is available. This situation arises, for instance, when the available right-hand side is determined by measurements. We will assume that y^δ satisfies

$$\|y - y^\delta\|_{\mathcal{Y}} \leq \delta$$

with a known bound $\delta > 0$.

The availability of y^δ instead of y suggests that we should seek to compute an approximate solution \tilde{x} of the equation

$$Tx = y^\delta, \quad x \in \mathcal{X}, \quad y^\delta \in \mathcal{Y}, \quad (2)$$

such that \tilde{x} is an accurate approximation of x^\dagger . Here we tacitly assume that the equation (2) is solvable. Note that equations of the form (2) arise in many applications including remote sensing [1], atmospheric tomography [36], computerized tomography [32], adaptive optics [34], and image restoration [4].

Since T is not continuously invertible, the least-squares solution of minimal norm of (2) typically is not a useful approximation of the solution x^\dagger of (1). To be able to determine an accurate approximation of x^\dagger from (2), the latter equation has to be *regularized*, i.e., the operator T has to be replaced with a nearby operator so that the solution of the equation so obtained is less sensitive to the error in y^δ than the solution of (2).

Much of the literature on the solution of operator equations (2) focuses on the analysis of these problems in infinite-dimensional Hilbert spaces, but properties of the finite-dimensional problems that arise through discretization before solution often are ignored. Conversely, many contributions to the literature on solution techniques for large-scale discretized problems obtained from (2) do not take into account the effects of the discretization error and of the approximation errors that stems from reducing the dimension of a large-scale discretized problem to a problem of smaller size. Among the exceptions are the papers [6, 35], which use results by Natterer [31] and Neubauer [33] to address this gap within the framework of Arnoldi-Tikhonov methods. These methods apply a few steps of the Arnoldi process to reduce the generally large matrix that is obtained when discretizing equation (2) to a linear system of algebraic equations with a matrix of small size. Applications of the Arnoldi process to the solution of large linear systems of equations that arise from the discretization of equations of the form (2), without discussing the effect of the discretization, are described in, e.g., [2, 15, 25, 30].

The main attraction of the Arnoldi process, when compared to the Golub-Kahan process to be discussed in this paper, is that the Arnoldi process does not require access to the transpose of the system matrix that is to be reduced, while the Golub-Kahan process does. This feature of the Arnoldi process makes it possible to reduce matrices for which matrix-vector products are easy to evaluate, but for which matrix-vector products with the transposed matrix are not. This situation may arise when the matrix is not explicitly formed, such as when the matrix is implicitly defined by a multipole method; see, e.g., [28]. Moreover, the Arnoldi process may require fewer matrix-vector product evaluations than the Golub-Kahan reduction methods, because the latter requires matrix-vector product evaluations with both the matrix and its transpose in every step; see [14] for an illustration. However, there are operator equations (2) for which the Arnoldi process is known to furnish poor results, such as when the operator T models motion blur and the desired solution x^\dagger is the blur- and noise-free image associated with an available blur- and noise-contaminated image y^δ ; see [18] for a computed example in finite dimensions. For some image restoration problems, it is possible to mitigate this difficulty by preconditioning; see [12]. Nevertheless, the difficulty of solving certain operator equations by reducing the associated discretized equation to a problem of small size by the Arnoldi process makes the Golub-Kahan process the default method for reducing a large linear system of algebraic equations to a system of small dimension; see, e.g., [4, 7, 8, 16, 25] for discussions and illustrations of this method.

The Golub-Kahan bidiagonalization process can be applied in Hilbert space and bounds for the error incurred by carrying out only a few steps with this process when applied to the solution of (2) are described in [3]. This analysis does not use results by Natterer [31]. The present paper applies bounds derived by Natterer to estimate the influence of the discretization error. We consider iterated Tikhonov regularization based on partial Golub-Kahan bidiagonalization instead of standard (non-iterated) Tikhonov regularization, because the former regularization method typically gives approximations of the desired solution x^\dagger of (1) of higher quality. Illustrations of the superior quality of approximate solutions computed by iterated Tikhonov methods applied to discretized problems can be found in, e.g., [5, 11, 12, 13, 17, 29]. When only one iteration of the iterated Golub-Kahan Tikhonov method is carried out, the method reduces to the classical Golub-Kahan-Tikhonov method.

It is the purpose of the present paper to analyze the effect of the discretization error and the error that stems from the dimension reduction achieved with the Golub-Kahan process on the computed solution determined by iterated Tikhonov regularization for the approximate solution of equation (2). Our analysis parallels that in [6], which concerns iterated Tikhonov regularization based on partial Arnoldi decomposition of the operator T . As we will see, some of the bounds derived in [6] also apply to the iterated Golub-Kahan-Tikhonov method of the present paper. Our analysis, which is based on work by Neubauer [33], suggests a new approach to determining the regularization parameter.

This paper is organized as follows. Section 2 discusses the discretization of equation (2) and introduces the iterated Tikhonov method. Section 3 recalls the iterated Arnoldi-Tikhonov method defined in [6]. The Golub-Kahan-Tikhonov method is reviewed in Section 4, and Section 5 describes our iterated Golub-Kahan-Tikhonov method and provides

convergence results. An alternative parameter choice method is discussed in Section 6 and a few computed examples are presented in Section 7. Concluding remarks can be found in Section 8.

We conclude this section with some comments on the work by Björck and Eldén on the Golub-Kahan-Tikhonov method. They were among the first to discuss this solution method for linear discrete ill-posed problems; see, e.g., [7, 8, 9, 19, 20, 21, 22]. Their work has had significant impact on later developments of solution methods for this kind of problems.

2 Preliminaries

Let T^\dagger stand for the Moore-Penrose pseudo-inverse of the operator T in (1) with

$$T^\dagger: \text{dom}(T^\dagger) \subseteq \mathcal{Y} \rightarrow \mathcal{X}, \quad \text{where } \text{dom}(T^\dagger) = \text{Rg}(T) \oplus \text{Rg}(T)^\perp.$$

For any $y \in \text{dom}(T^\dagger)$, the element $x^\dagger := T^\dagger y$ is the unique least-square solution of minimal norm of equation (1). To ensure consistency in (1), we will assume that

$$y \in \text{dom}(T^\dagger).$$

Since T is not continuously invertible, the operator T^\dagger is unbounded. This may make the least-squares solution $T^\dagger y$ of (1) very sensitive to the error in y^δ . A regularization method replaces T^\dagger by a member of a family $\{R_\alpha: \mathcal{Y} \rightarrow \mathcal{X}\}$ of continuous operators that depend on a parameter α , paired with a suitable parameter choice rule $\alpha = \alpha(\delta, y^\delta) > 0$. The pair (R_α, α) furnishes a point-wise approximation of T^\dagger ; see [23, Definition 3.1] for a rigorous definition.

2.1 Discretization and Tikhonov regularization

When to compute an approximate least-squares solution of (2), we first discretize the equation and then compute an approximate solution of the discretized equation obtained. The discretization introduces a discretization error. To bound the propagated discretization error, we use results by Natterer [31] following a similar approach as in [35].

Consider a sequence $\mathcal{X}_1 \subset \mathcal{X}_2 \subset \dots \subset \mathcal{X}_n \subset \dots \subset \mathcal{X}$ of finite-dimensional subspaces \mathcal{X}_n of \mathcal{X} with $\dim(\mathcal{X}_n) < \infty$, whose union is dense in \mathcal{X} . Define the projectors $P_n: \mathcal{X} \rightarrow \mathcal{X}_n$ and $Q_n: \mathcal{Y} \rightarrow \mathcal{Y}_n := T(\mathcal{X}_n)$, as well as the inclusion operator $\iota_n: \mathcal{X}_n \hookrightarrow \mathcal{X}$. Application of these operators to equations (1) and (2) gives the equations

$$\begin{aligned} Q_n T \iota_n P_n x &= Q_n y, \\ Q_n T \iota_n P_n x &= Q_n y^\delta. \end{aligned}$$

Introduce the operator $T_n: \mathcal{X}_n \rightarrow \mathcal{Y}_n$,

$$T_n := Q_n T \iota_n,$$

and the finite-dimensional vectors

$$y_n := Q_n y, \quad y_n^\delta := Q_n y^\delta, \quad x_n := P_n x.$$

It is natural to identify T_n with a matrix in $\mathbb{R}^{n_1 \times n_2}$ with $n_2 = \dim(\mathcal{X}_n)$, $n_1 = \dim(\mathcal{Y}_n)$, and y_n , y_n^δ , and x_n with elements in \mathbb{R}^{n_1} and \mathbb{R}^{n_2} , respectively. This gives us the linear systems of equations

$$T_n x_n = y_n, \tag{3}$$

$$T_n x_n = y_n^\delta. \tag{4}$$

Henceforth, we will consider T_n a matrix that represents a discretization of T .

Let T_n^\dagger denote the Moore-Penrose pseudo-inverse of the matrix T_n . Then the unique least-squares solutions with respect to the Euclidean vector norm of equations (3) and (4) are given by

$$x_n^\dagger := T_n^\dagger y_n \quad \text{and} \quad x_n^{\dagger, \delta} := T_n^\dagger y_n^\delta,$$

respectively. The fact that the operator T has an unbounded inverse results in that the matrix T_n is singular or severely ill-conditioned. It follows that $x_n^{\dagger, \delta}$ may be a useless approximation of x_n^\dagger . We conclude that regularization of the discretized operator equation (4) is required.

Note that the solution $x_n^\dagger \in \mathcal{X}_n$ of (3) might not be an accurate approximation of the solution x^\dagger of (1), due to a large propagated discretization error. We therefore are interested in determining a bound for $\|x^\dagger - x_n^\dagger\|_{\mathcal{X}}$. This, in general,

requires some additional assumptions. In particular, it is not sufficient for T and T_n to be close in the operator norm; see [23, Example 3.19]. We will assume that

$$\|x^\dagger - x_n^\dagger\|_{\mathcal{X}} \leq f(n) \rightarrow 0 \quad \text{as } n \rightarrow \infty, \quad (\text{H1})$$

for a suitable function f . For instance, if T is compact and $\limsup_{n \rightarrow \infty} \|T_n^* x_n^\dagger\|_{\mathcal{X}} < \infty$, where the superscript $*$ stands for matrix transposition, or if T is compact and $\{\mathcal{X}_n\}_n$ is a discretization resulting from the *dual-least square projection* method, see [23, Section 3.3], then

$$f(n) = O(\|(I - P_n)T^*\|),$$

where $\|\cdot\|$ denotes the operator norm induced by the norms $\|\cdot\|_{\mathcal{X}}$ and $\|\cdot\|_{\mathcal{Y}}$.

We conclude this subsection by letting $\{e_j\}_{j=1}^{n_2}$ be a convenient basis for \mathcal{X}_n . Consider the representation

$$x_n = \sum_{j=1}^{n_2} x_j^{(n)} e_j$$

of an element $x_n \in \mathcal{X}_n$ and identify x_n with the vector

$$\mathbf{x}_n = [x_1^{(n)}, \dots, x_{n_1}^{(n)}]^* \in \mathbb{R}^{n_2}.$$

If $\{e_j\}_{j=1}^{n_2}$ is an orthonormal basis, then we may choose the norms so that $\|\mathbf{x}_n\|_2 = \|x_n\|_{\mathcal{X}}$. Here and throughout this paper $\|\cdot\|_2$ denotes the Euclidean vector norm. However, for certain discretization methods, the basis $\{e_j\}_{j=1}^{n_2}$ is not orthonormal and this equality does not hold. Following [35], we then assume that there are positive constants c_{\min} and c_{\max} , independent of n , such that

$$c_{\min} \|\mathbf{x}_n\|_2 \leq \|x_n\|_{\mathcal{X}} \leq c_{\max} \|\mathbf{x}_n\|_2. \quad (\text{H2})$$

Such inequalities hold in many practical situations, e.g., when using B-splines, wavelets, and the discrete cosine transform; see [10, 27].

Due to the ill-conditioning of the matrix T_n in (4), the least-squares solution of (4) of minimal norm $x_n^{\dagger, \delta}$ generally is not a useful approximation of the minimal norm solution x_n^\dagger of (3). Therefore, the operator T_n^\dagger has to be replaced with a nearby operator that is less sensitive to the error in y^δ . A common replacement is furnished by Tikhonov regularization which, when applied to (4), reads

$$x_{\alpha, n}^\delta := \operatorname{argmin}_{x_n \in \mathbb{R}^{n_2}} \|T_n x_n - y_n^\delta\|_2^2 + \alpha \|x_n\|_2^2.$$

The regularization parameter $\alpha > 0$ determines the amount of regularization. The Tikhonov solution $x_{\alpha, n}^\delta$ can be expressed as

$$x_{\alpha, n}^\delta = (T_n^* T_n + \alpha I_n)^{-1} T_n^* y_n^\delta, \quad (5)$$

where I_n denotes the identity matrix of order n .

A generalized version of this method is the iterated Tikhonov method, which is known to give a better approximation of the desired solution x_n^\dagger . The closed form formula for the i -th approximation given by this method is

$$x_{\alpha, n, i}^\delta = \sum_{k=1}^i \alpha^{k-1} (T_n^* T_n + \alpha I_n)^{-k} T_n^* y_n^\delta. \quad (6)$$

Thus, the Tikhonov solution (5) corresponds to $i = 1$.

Clearly, when n is large, computing $x_{\alpha, n, i}^\delta$ by formula (6), or $x_{\alpha, n}^\delta = x_{\alpha, n, 1}^\delta$ by formula (5), is impractical. This work discusses how to reduce the complexity of iterated Tikhonov regularization and achieve a fairly accurate approximation of $x_{\alpha, n, i}^\delta$ by applying a few steps of Golub-Kahan bidiagonalization to the matrix T_n with initial vector y_n^δ .

3 The iterated Arnoldi-Tikhonov method

We briefly recall the iterated Arnoldi-Tikhonov (iAT) method presented in [6], which uses a partial Arnoldi decomposition instead of a partial Golub-Kahan bidiagonalization to implement the iterated Tikhonov method (6), because some results for the iAT method carry over to the iterated Golub-Kahan Tikhonov (iGKT) method and because we will compare the performance of these methods. We assume in this section that $n = n_1 = n_2$.

Application of $1 \leq \ell \ll n$ steps of the Arnoldi process to the square matrix T_n with initial vector y_n^δ generically gives the Arnoldi decomposition

$$T_n V_{n,\ell} = V_{n,\ell+1} H_{\ell+1,\ell}.$$

The columns of the matrix

$$V_{n,\ell+1} = \left[v_{n,\ell+1}^{(1)} \mid \cdots \mid v_{n,\ell+1}^{(\ell+1)} \right] = \left[V_{n,\ell} \mid v_{n,\ell+1}^{(\ell+1)} \right] \in \mathbb{R}^{n_1 \times (\ell+1)}$$

form an orthonormal basis for the Krylov subspace

$$\mathcal{K}_{\ell+1}(T_n, y_n^\delta) = \text{span}\{y_n^\delta, T_n y_n^\delta, \dots, T_n^\ell y_n^\delta\}.$$

Moreover, $H_{\ell+1,\ell} \in \mathbb{R}^{(\ell+1) \times \ell}$ is an upper Hessenberg matrix, i.e., all entries below the subdiagonal vanish. We will assume the generic situation that all subdiagonal entries of $H_{\ell+1,\ell}$ are nonvanishing. This requirement can easily be removed.

Define the Arnoldi approximation

$$\tilde{T}_n^{(\ell)} := V_{n,\ell+1} H_{\ell+1,\ell} V_{n,\ell}^* \in \mathbb{R}^{n \times n}, \quad (7)$$

of the matrix T_n . We will assume that

$$\|T_n - \tilde{T}_n^{(\ell)}\|_2 \leq \tilde{h}_\ell \quad \text{for some} \quad \tilde{h}_\ell \geq 0.$$

Notice that when $\ell = n$, we have $\tilde{T}_n^{(n)} = T_n$.

We apply the iterated Tikhonov regularization (6) with the approximation (7). Convergence results obtained in [6] are analogous to the ones in Section 5. We summarize the iAT method in Algorithm 1.

Algorithm 1 The iAT method

Input: $\{T_n, y_n^\delta, \ell, i\}$

Output: $\tilde{x}_{\tilde{\alpha},n,i}^{\delta,\ell}$

- 1: Compute $\{V_{n,\ell+1}, H_{\ell+1,\ell}\}$ with the Arnoldi process [37, Section 6.3]
 - 2: Compute $\tilde{y}_{\ell+1}^\delta = V_{n,\ell+1}^* y_n^\delta$
 - 3: Set $\tilde{\alpha}$
 - 4: Compute $\tilde{z}_{\tilde{\alpha},\ell,i}^{\delta,\ell} = \sum_{k=1}^i \tilde{\alpha}^{k-1} (H_{\ell+1,\ell}^* H_{\ell+1,\ell} + \tilde{\alpha} I_\ell)^{-k} H_{\ell+1,\ell}^* \tilde{y}_{\ell+1}^\delta$
 - 5: Return $\tilde{x}_{\tilde{\alpha},n,i}^{\delta,\ell} = V_{n,\ell} \tilde{z}_{\tilde{\alpha},\ell,i}^{\delta,\ell}$
-

In order to compute the parameter $\tilde{\alpha}$ as proposed in [6], we define the operator $\tilde{\mathcal{R}}_\ell$ to be the orthogonal projector from \mathbb{R}^n into $\text{Rg}(\tilde{T}_n^{(\ell)})$. Let $\tilde{q} = \text{rank}(H_{\ell+1,\ell})$ and introduce the singular value decomposition

$$H_{\ell+1,\ell} = \tilde{W}_{\ell+1} \tilde{\Sigma}_{\ell+1,\ell} \tilde{S}_\ell^*,$$

where the matrices $\tilde{W}_{\ell+1} \in \mathbb{R}^{(\ell+1) \times (\ell+1)}$ and $\tilde{S}_\ell \in \mathbb{R}^{\ell \times \ell}$ are orthogonal, and the diagonal entries of the matrix

$$\tilde{\Sigma}_{\ell+1,\ell} = \text{diag}[\tilde{\sigma}_1, \tilde{\sigma}_2, \dots, \tilde{\sigma}_\ell] \in \mathbb{R}^{(\ell+1) \times \ell}$$

are ordered according to $\tilde{\sigma}_1 \geq \dots \geq \tilde{\sigma}_{\tilde{q}} > \tilde{\sigma}_{\tilde{q}+1} = \dots = \tilde{\sigma}_\ell = 0$. Since all subdiagonal entries of the matrix $H_{\ell+1,\ell}$ are nonvanishing, the matrix has full rank $\tilde{q} = \ell$. Let

$$I_{\ell,\ell+1} = \begin{bmatrix} I_\ell & 0 \\ 0 & 0 \end{bmatrix} \in \mathbb{R}^{(\ell+1) \times (\ell+1)},$$

then

$$\tilde{\mathcal{R}}_\ell = V_{n,\ell+1} \tilde{W}_{\ell+1} I_{\ell,\ell+1} \tilde{W}_{\ell+1}^* V_{n,\ell+1}^*.$$

Define

$$\tilde{y}_{\ell+1}^\delta := I_{\ell,\ell+1} \tilde{W}_{\ell+1}^* \tilde{y}_{\ell+1}^\delta$$

and assume that at least one of the first \tilde{q} entries of the vector $\tilde{y}_{\ell+1}^\delta$ is non-vanishing. Then the equation

$$\tilde{\alpha}^{2i+1} (\tilde{y}_{\ell+1}^\delta)^* (\tilde{\Sigma}_{\ell+1,\ell} \tilde{\Sigma}_{\ell+1,\ell}^* + \tilde{\alpha} I_{\ell+1})^{-2i-1} \tilde{y}_{\ell+1}^\delta = (E \tilde{h}_\ell + C \delta)^2, \quad (8)$$

possesses a unique solution $\tilde{\alpha} > 0$ if we choose positive constants C and E such that

$$0 \leq E \tilde{h}_\ell + C \delta \leq \|\tilde{\mathcal{R}}_\ell \tilde{y}_n^\delta\|_2 = \|I_{\ell,\ell+1} \tilde{W}_{\ell+1}^* \tilde{y}_{\ell+1}^\delta\|_2. \quad (9)$$

We recall the main results of [6].

Proposition 1. [6, Proposition 1] Set $C = 1$ and $E = \|x_n^\dagger\|_2$ in equation (8). Let equation (9) hold and let $\tilde{\alpha} > 0$ be the unique solution of (8). Then for all $\hat{\alpha} \geq \tilde{\alpha}$, we have that $\|x_n^\dagger - \tilde{x}_{\hat{\alpha},n,i}^{\delta,\ell}\|_2 \leq \|x_n^\dagger - \tilde{x}_{\tilde{\alpha},n,i}^{\delta,\ell}\|_2$.

Proposition 2. [6, Proposition 2] Set $C = 1$ and $E = \|x_n^\dagger\|_2$ in equation (8). Let equation (9) hold and let $\tilde{\alpha} > 0$ be the unique solution of (8). For some $\nu \geq 0$ and $\rho > 0$, let $x_n^\dagger \in \mathcal{X}_{n,\nu,\rho}$, where

$$\mathcal{X}_{n,\nu,\rho} := \{x_n \in \mathcal{X}_n \mid x_n = (T_n^* T_n)^\nu w_n, w_n \in \ker(T_n)^\perp \text{ and } \|w_n\|_2 \leq \rho\}.$$

Then

$$\|x_n^\dagger - \tilde{x}_{\tilde{\alpha},n,i}^{\delta,\ell}\|_2 = \begin{cases} o(1) & \text{if } \nu = 0, \\ o((h_\ell + \delta)^{\frac{2\nu i}{2\nu i + 1}}) + O(\gamma_\ell^{2\nu} \|w_n\|_2) & \text{if } 0 < \nu < 1, \\ O((h_\ell + \delta)^{\frac{2i}{2i+1}}) + O(\gamma_\ell \|(I_n - \tilde{R}_\ell)T_n w_n\|_2) & \text{if } \nu = 1, \end{cases}$$

where $\gamma_\ell := \|(I_n - \tilde{R}_\ell)T_n\|_2$.

Corollary 3. Assume that $x_n^\dagger \in \mathcal{X}_{n,1,\rho}$ and let $\tilde{\alpha} > 0$ be the solution of (8). Then for ℓ such that $\tilde{h}_\ell \sim \delta$, we have

$$\begin{aligned} \|x_n^\dagger - \tilde{x}_{\tilde{\alpha},n,i}^{\delta,\ell}\|_2 &= O(\delta^{\frac{2i}{2i+1}}) \quad \text{as } \delta \rightarrow 0, \\ \|x_n^\dagger - \tilde{x}_{\tilde{\alpha},n,i}^{\delta,\ell}\|_{\mathcal{X}} &\leq f(n) + O(\delta^{\frac{2i}{2i+1}}) \quad \text{as } \delta \rightarrow 0. \end{aligned}$$

As discussed at the end of [6, Appendix A.2], if an estimate of $\|x_n^\dagger\|_2$ is not available, then we may substitute E by the expression $D\|\tilde{x}_{\tilde{\alpha},n,i}^{\delta,\ell}\|_2$, with a constant $D \geq 1$. With this choice, for $\tilde{\alpha}$ satisfying (9), we achieve the same convergence rates.

4 The Golub-Kahan-Tikhonov method

Golub-Kahan bidiagonalization is a commonly used technique to reduce a large matrix to a small one, while retaining some of the important characteristics of the large matrix. This section reviews the Golub-Kahan bidiagonalization method and shows how it can be applied to approximate the discretized equation (4) and its Tikhonov regularized solution (5) in a low-dimensional subspace \mathbb{R}^ℓ with $1 \leq \ell \ll \min\{n_1, n_2\}$. Thorough discussions of the Golub-Kahan decomposition can be found in Björck [8] and in Golub and Van Loan [26]. Applications to Tikhonov regularization are discussed, e.g., in [7, 16, 25].

Algorithm 2 Golub-Kahan bidiagonalization

Input: matrix $T_n \in \mathbb{R}^{n_1 \times n_2}$, number of steps $1 \leq \ell \ll \min\{n_1, n_2\}$, initial vector $y_n^\delta \in \mathbb{R}^{n_2}$

Output: lower bidiagonal matrix $B_{\ell+1,\ell} \in \mathbb{R}^{(\ell+1) \times \ell}$, matrices

$U_{\ell+1} = [u_1, u_2, \dots, u_{\ell+1}] \in \mathbb{R}^{n_1 \times (\ell+1)}$ and $V_\ell = [v_1, v_2, \dots, v_\ell] \in \mathbb{R}^{n_2 \times \ell}$ with orthonormal columns

- 1: $\beta_1 = \|y_n^\delta\|_2; u_1 = y_n^\delta / \beta_1; v_0 = 0;$
 - 2: **for** $i = 1$ **to** ℓ **do**
 - 3: $w = T_n^* u_i - \beta_i v_{i-1};$
 - 4: $\alpha_i = \|w\|_2; v_i = w / \alpha_i; B_{i,i} = \alpha_i$
 - 5: $w = T_n v_i - \alpha_i u_i$
 - 6: $\beta_{i+1} = \|w\|_2; u_{i+1} = w / \beta_{i+1}; B_{i+1,i} = \beta_{i+1}$
 - 7: **end for**
-

Generically, Algorithm 2 determines the Golub-Kahan decompositions

$$T_n V_\ell = U_{\ell+1} B_{\ell+1,\ell} \quad \text{and} \quad T_n^* U_\ell = V_\ell B_{\ell,\ell}^*, \quad (10)$$

where $V_\ell \in \mathbb{R}^{n_2 \times \ell}$, the matrix $U_\ell \in \mathbb{R}^{n_1 \times \ell}$ is made up of the first ℓ columns of $U_{\ell+1} \in \mathbb{R}^{n_1 \times (\ell+1)}$ and the matrix $B_{\ell,\ell} \in \mathbb{R}^{\ell \times \ell}$ consists of the first ℓ rows of the lower bidiagonal matrix

$$B_{\ell+1,\ell} = \begin{bmatrix} \alpha_1 & 0 & \cdots & 0 \\ \beta_2 & \alpha_2 & 0 & \cdots & \vdots \\ 0 & \beta_3 & \ddots & & \\ \vdots & & \ddots & \alpha_{\ell-1} & 0 \\ 0 & \cdots & & \beta_\ell & \alpha_\ell \\ 0 & \cdots & & & \beta_{\ell+1} \end{bmatrix} \in \mathbb{R}^{(\ell+1) \times \ell}.$$

We will assume the generic situation that all nontrivial entries of $B_{\ell+1,\ell}$ are nonvanishing.

Moreover, we have

$$\begin{aligned} \text{span}\{u_1, u_2, \dots, u_{\ell+1}\} &= \text{span}\{y_n^\delta, T_n T_n^* y_n^\delta, \dots, (T_n T_n^*)^\ell y_n^\delta\}, \\ \text{span}\{v_1, v_2, \dots, v_\ell\} &= \text{span}\{T_n^* y_n^\delta, (T_n^* T_n) T_n^* y_n^\delta, \dots, (T_n T_n^*)^{\ell-1} T_n^* y_n^\delta\}. \end{aligned}$$

Define the Golub-Kahan approximation

$$T_n^{(\ell)} := U_{\ell+1} B_{\ell+1,\ell} V_\ell^* \in \mathbb{R}^{n_1 \times n_2} \quad (11)$$

of the matrix T_n . We will assume that

$$\|T_n - T_n^{(\ell)}\|_2 \leq h_\ell \quad \text{for some } h_\ell \geq 0.$$

Note that when $\ell = \min\{n_1, n_2\}$ in Algorithm 2, we have $T_n^{(\ell)} = T_n$.

Having the Golub-Kahan approximation (11) makes it possible to solve the *approximated* discretized equation

$$T_n^{(\ell)} x_n = y_n^\delta \quad (12)$$

instead of the discretized equation (4). This is beneficial because a solution of equation (12) can be computed much faster than a solution of (4) when the matrix T_n is large.

Application of Tikhonov regularization (5) to equation (12) gives the solution

$$x_{\alpha,n}^{\delta,\ell} := (T_n^{(\ell)*} T_n^{(\ell)} + \alpha I_n)^{-1} T_n^{(\ell)*} y_n^\delta. \quad (13)$$

We exploit the structure of $T_n^{(\ell)}$ to reduce the computational complexity of computing the solution (13). For any $x_\ell \in \mathbb{R}^\ell$, we have

$$\begin{aligned} V_\ell(B_{\ell+1,\ell}^* B_{\ell+1,\ell} + \alpha I_\ell) x_\ell &= (V_\ell B_{\ell+1,\ell}^* U_{\ell+1}^* U_{\ell+1} B_{\ell+1,\ell} V_\ell^* + \alpha I_n) V_\ell x_\ell \\ &= (T_n^{(\ell)*} T_n^{(\ell)} + \alpha I_n) V_\ell x_\ell \end{aligned}$$

and, therefore,

$$(T_n^{(\ell)*} T_n^{(\ell)} + \alpha I)^{-1} V_\ell = V_\ell (B_{\ell+1,\ell}^* B_{\ell+1,\ell} + \alpha I_\ell)^{-1}. \quad (14)$$

Let $y_{\ell+1}^\delta := U_{\ell+1}^* y_n^\delta \in \mathbb{R}^{\ell+1}$. Then

$$z_{\alpha,\ell}^{\delta,\ell} := (B_{\ell+1,\ell}^* B_{\ell+1,\ell} + \alpha I_\ell)^{-1} B_{\ell+1,\ell}^* y_{\ell+1}^\delta$$

is the Tikhonov regularized solution associated with the *reduced* discretized equation

$$B_{\ell+1,\ell} z_\ell = y_{\ell+1}^\delta.$$

Combining equations (11), (13), and (14), we obtain

$$x_{\alpha,n}^{\delta,\ell} = V_\ell z_{\alpha,\ell}^{\delta,\ell}.$$

This procedure of computing an approximate solution of (4), and therefore of (2), is referred to as the *Golub-Kahan-Tikhonov (GKT) regularization method*. Algorithm 3 summarizes the computations. We will comment on the choice of the regularization parameter $\alpha > 0$ below.

Algorithm 3 The Golub-Kahan-Tikhonov regularization method

Input: T_n, y_n^δ, ℓ

Output: $x_{\alpha,n}^{\delta,\ell}$

- 1: Compute the matrices $U_{\ell+1}$, V_ℓ , and $B_{\ell+1,\ell}$ with Algorithm 2
 - 2: Compute $y_{\ell+1}^\delta = U_{\ell+1}^* y_n^\delta$
 - 3: Set α
 - 4: Compute $z_{\alpha,\ell}^{\delta,\ell} = (B_{\ell+1,\ell}^* B_{\ell+1,\ell} + \alpha I_\ell)^{-1} B_{\ell+1,\ell}^* y_{\ell+1}^\delta$
 - 5: Compute $x_{\alpha,n}^{\delta,\ell} = V_\ell z_{\alpha,\ell}^{\delta,\ell}$
-

A convergence analysis for approximate solutions of (2) computed with Algorithm 3 is carried out in [3], where also convergence rates for $\|x_n^\dagger - x_{\alpha,n}^{\delta,\ell}\|_2$ are established. Convergence in the space \mathcal{X} then is obtained by using (H2).

5 The iterated Golub-Kahan-Tikhonov method

This section describes an iterated variant of the Golub-Kahan-Tikhonov regularization method outlined by Algorithm 3. We refer to this variant as the iterated Golub-Kahan-Tikhonov (iGKT) method and analyze its convergence properties. Our interest in the iGKT method stems from the fact that it delivers more accurate approximations of x^\dagger than the GKT method. A reason for this is that the standard (non-iterated) Tikhonov regularization method exhibits a saturation rate of $O(\delta^{2/3})$ as $\delta \searrow 0$, as shown in [23, Proposition 5.3]. It follows that approximate solutions computed with the GKT method do not converge to the solution of (2) faster than $O(\delta^{2/3})$ as $\delta \searrow 0$. However, the iGKT method can surpass this saturation rate, as is shown in Corollary 6 below. We remark that the computational effort required by the iGKT method is essentially the same as for the non-iterated GKT method.

5.1 Definition of the iGKT method

The GKT method is combined with iterated Tikhonov regularization (6) using the matrix $T_n^{(\ell)}$ in (11). This yields the iterative method

$$x_{\alpha,n,i}^{\delta,\ell} = \sum_{k=1}^i \alpha^{k-1} (T_n^{(\ell)*} T_n^{(\ell)} + \alpha I_n)^{-k} T_n^{(\ell)*} y_n^\delta. \quad (15)$$

We will denote the left-hand side by $x_{\alpha,n,i}^\ell$ when the vector y_n^δ is replaced by y_n . Similarly as in Algorithm 3, it follows from the Golub-Kahan decomposition that

$$x_{\alpha,n,i}^{\delta,\ell} = V_\ell z_{\alpha,\ell,i}^{\delta,\ell},$$

where

$$z_{\alpha,\ell,i}^{\delta,\ell} := \sum_{k=1}^i \alpha^{k-1} (B_{\ell+1,\ell}^* B_{\ell+1,\ell} + \alpha I_\ell)^{-k} B_{\ell+1,\ell}^* y_{\ell+1}^\delta.$$

The iGKT method is described by Algorithm 4. Step 4 of the algorithm is evaluated by using an iteration analogous to (15) and computing the Cholesky factorization of the matrix $B_{\ell+1,\ell}^* B_{\ell+1,\ell} + \alpha I_\ell$. Notice that for $i = 1$, we recover the GKT method of Algorithm 3. Assume that the matrix T_n is large and that $\ell \ll \min\{n_1, n_2\}$. This is a situation of interest to us. Then the main computational effort required by Algorithm 4 is the evaluation of ℓ matrix-vector products with each one of the matrices T_n and T_n^* needed to calculate the Golub-Kahan decomposition (10). Note that the computational effort required by Algorithm 4 is essentially independent of the number of iterations i of the iGKT method.

Algorithm 4 The iGKT method

Input: T_n, y_n^δ, ℓ, i

Output: $x_{\alpha,n,i}^{\delta,\ell}$

- 1: Compute the matrices $U_{\ell+1}$, V_ℓ , and $B_{\ell+1,\ell}$ with Algorithm 2
 - 2: Compute $y_{\ell+1}^\delta = U_{\ell+1}^* y_n^\delta$
 - 3: Set α
 - 4: Compute $z_{\alpha,\ell,i}^{\delta,\ell} = \sum_{k=1}^i \alpha^{k-1} (B_{\ell+1,\ell}^* B_{\ell+1,\ell} + \alpha I_\ell)^{-k} B_{\ell+1,\ell}^* y_{\ell+1}^\delta$
 - 5: Compute $x_{\alpha,n,i}^{\delta,\ell} = V_\ell z_{\alpha,\ell,i}^{\delta,\ell}$
-

5.2 Convergence results

This section discusses some convergence results for the iGKT method described by Algorithm 4. The results parallel those shown for the iAT method in [6]. They only differ in that, in the present paper, we define the Golub-Kahan approximation (11) of the matrix T_n , while in [6] the analogous approximation (7) is defined by using a partial Arnoldi decomposition of T_n . In particular, the proofs presented in [6] carry over to the setting of the present paper. Therefore, when presenting the convergence analysis, we refer to [6] for proofs. Our results are based on work by Neubauer [33]. This connection is clear in the Appendix of [6].

We will need the orthogonal projector \mathcal{R}_ℓ from \mathbb{R}^{n_1} into $\text{Rg}(T_n^{(\ell)})$. Let $q = \text{rank}(B_{\ell+1,\ell})$ and introduce the singular value decomposition

$$B_{\ell+1,\ell} = W_{\ell+1} \Sigma_{\ell+1,\ell} S_\ell^*,$$

where the matrices $W_{\ell+1} \in \mathbb{R}^{(\ell+1) \times (\ell+1)}$ and $S_\ell \in \mathbb{R}^{\ell \times \ell}$ are orthogonal, and the diagonal entries of the matrix

$$\Sigma_{\ell+1,\ell} = \text{diag}[\sigma_1, \sigma_2, \dots, \sigma_\ell] \in \mathbb{R}^{(\ell+1) \times \ell}$$

are ordered according to $\sigma_1 \geq \dots \geq \sigma_q > \sigma_{q+1} = \dots = \sigma_\ell = 0$. Since we assume the Golub-Kahan process does not break down, the matrix $B_{\ell+1,\ell}$ has full rank $q = \ell$. Let

$$I_{\ell,\ell+1} = \begin{bmatrix} I_\ell & 0 \\ 0 & 0 \end{bmatrix} \in \mathbb{R}^{(\ell+1) \times (\ell+1)}.$$

Then

$$\mathcal{R}_\ell = U_{\ell+1} W_{\ell+1} I_{\ell,\ell+1} W_{\ell+1}^* U_{\ell+1}^*.$$

Define

$$\hat{y}_{\ell+1}^\delta := I_{\ell,\ell+1} W_{\ell+1}^* y_{\ell+1}^\delta$$

and assume that at least one of the first q entries of the vector $\hat{y}_{\ell+1}^\delta$ is non-vanishing. Then the equation

$$\alpha^{2i+1} (\hat{y}_{\ell+1}^\delta)^* (\Sigma_{\ell+1,\ell} \Sigma_{\ell+1,\ell}^* + \alpha I_{\ell+1})^{-2i-1} \hat{y}_{\ell+1}^\delta = (E h_\ell + C \delta)^2, \quad (16)$$

with positive constants C and E has a unique solution $\alpha > 0$ if we choose C and E so that

$$0 \leq E h_\ell + C \delta \leq \|\mathcal{R}_\ell y_n^\delta\|_2 = \|I_{\ell,\ell+1} W_{\ell+1}^* y_{\ell+1}^\delta\|_2. \quad (17)$$

By using the same techniques as for Propositions 1 and 2 and Corollary 3 respectively, we obtain the following results.

Proposition 4. Set $C = 1$ and $E = \|x_n^\dagger\|_2$ in equation (16). Let equation (17) hold and let $\alpha > 0$ be the unique solution of (16). Then for all $\hat{\alpha} \geq \alpha$, we have that $\|x_n^\dagger - x_{\alpha,n,i}^{\delta,\ell}\|_2 \leq \|x_n^\dagger - x_{\hat{\alpha},n,i}^{\delta,\ell}\|_2$.

Proposition 5. Set $C = 1$ and $E = \|x_n^\dagger\|_2$. Assume that (17) holds and let $\alpha > 0$ be the unique solution of (16). For some $\nu \geq 0$ and $\rho > 0$, let $x_n^\dagger \in \mathcal{X}_{n,\nu,\rho}$, where

$$\mathcal{X}_{n,\nu,\rho} := \{x_n \in \mathcal{X}_n \mid x_n = (T_n^* T_n)^\nu w_n, w_n \in \ker(T_n)^\perp \text{ and } \|w_n\|_2 \leq \rho\}.$$

Then

$$\|x_n^\dagger - x_{\alpha,n,i}^{\delta,\ell}\|_2 = \begin{cases} o(1) & \text{if } \nu = 0, \\ o((h_\ell + \delta)^{\frac{2\nu i}{2\nu i + 1}}) + O(\gamma_\ell^{2\nu} \|w_n\|_2) & \text{if } 0 < \nu < 1, \\ O((h_\ell + \delta)^{\frac{2i}{2i+1}}) + O(\gamma_\ell \|(I_n - \mathcal{R}_\ell) T_n w_n\|_2) & \text{if } \nu = 1, \end{cases}$$

where $\gamma_\ell := \|(I_n - \mathcal{R}_\ell) T_n\|_2$.

Corollary 6. Assume that $x_n^\dagger \in \mathcal{X}_{n,1,\rho}$ and let $\alpha > 0$ be the solution of (16). Then, for ℓ such that $h_\ell \sim \delta$, we have

$$\begin{aligned} \|x_n^\dagger - x_{\alpha,n,i}^{\delta,\ell}\|_2 &= O(\delta^{\frac{2i}{2i+1}}) \quad \text{as } \delta \rightarrow 0, \\ \|x_n^\dagger - x_{\alpha,n,i}^{\delta,\ell}\|_{\mathcal{X}} &\leq f(n) + O(\delta^{\frac{2i}{2i+1}}) \quad \text{as } \delta \rightarrow 0. \end{aligned}$$

As mentioned at the end of Section 3, if an estimate of $\|x_n^\dagger\|_2$ is not available, then we may substitute E by the expression $D \|x_{\alpha,n,i}^{\delta,\ell}\|_2$ with a constant $D \geq 1$. With this choice, for α satisfying (17), we achieve the same convergence rates.

We note the improvement of the convergence rate $O(\delta^{2/3})$ for standard (non-iterated) Tikhonov regularization.

6 An alternative parameter choice strategy

In this section we describe a parameter choice strategy that differs from the one above. Our aim is to be able to determine more accurate approximations of the desired solution x^\dagger of (1) and to compute these solutions in lower-dimensional Krylov subspace. Our analysis requires that Assumption 1 holds. To enhance readability, we provide Table 1, which connects the notation used in this section with the notation used for the iAT and iGKT methods in the previous sections.

Assumption 1. Let $T: \mathcal{X} \rightarrow \mathcal{Y}$ denote a bounded linear operator between separable Hilbert spaces \mathcal{X} and \mathcal{Y} with norms $\|\cdot\|_{\mathcal{X}}$ and $\|\cdot\|_{\mathcal{Y}}$, respectively, that are induced by inner products, and let T_h be an approximation of T . Consider a family $\{W_m\}_{m \in \mathbb{N}}$ of finite-dimensional subspaces of \mathcal{Y} such that the orthogonal projector Q_m into W_m converges to I on $\overline{\text{Rg } T}$.

Notation of this section	T	T_h	Q_m	$T_{h,m} := Q_m T_h$	x^\dagger	$x_{\alpha,m,i}^{\delta,h}$
Notation of iAT	T_n	$\tilde{T}_n^{(\ell)}$	$\tilde{\mathcal{R}}_\ell$	$T_n^{(\ell)}$	x_n^\dagger	$\tilde{x}_{\alpha,n,i}^{\delta,\ell}$
Notation of iGKT	T_n	$T_n^{(\ell)}$	\mathcal{R}_ℓ	$T_n^{(\ell)}$	x_n^\dagger	$x_{\alpha,n,i}^{\delta,\ell}$

Table 1: Comparison of notation.

Define the operator $T_{h,m} := Q_m T_h$. Using the iterated Tikhonov (iT) method (see [23, Section 5]) applied to the solution of equation (2) with the operator $T_{h,m}$, we define the approximate solution

$$x_{\alpha,m,i}^{\delta,h} := \sum_{k=1}^i \alpha^{k-1} (T_{h,m}^* T_{h,m} + \alpha I)^{-k} T_{h,m}^* y^\delta \quad (18)$$

of (2). Consider for $\tau \geq 1$ the equation for α ,

$$\alpha^{2i+1} \langle (T_{h,m} T_{h,m}^* + \alpha I)^{-2i-1} Q_m y^\delta, Q_m y^\delta \rangle = \tau \delta^2. \quad (19)$$

Similarly as in [6, Proposition A.6], one can show that there is a unique solution α of (19) provided that

$$\tau \delta^2 < \|Q_m y^\delta\|^2. \quad (20)$$

Proposition 7. *Let Assumption 1 and (20) hold with $\tau = 1$. If $Q_m T x^\dagger = T_{h,m} x^\dagger$ and α is the unique solution of (19), then for all $\alpha' \geq \alpha$, we have $\|x^\dagger - x_{\alpha,m,i}^{\delta,h}\| \leq \|x^\dagger - x_{\alpha',m,i}^{\delta,h}\|$.*

Proof. Let $\{F_\mu^{h,m}\}_{\mu \in \mathbb{R}}$ be a spectral family for $T_{h,m} T_{h,m}^*$. We recall that for any self-adjoint operator A , there exists a unique spectral family $\{E_\mu\}_{\mu \in \mathbb{R}}$ that is a collection of projectors such that

$$f(A)x = \int_0^\infty f(\mu) dE_\mu x := \lim_{n \rightarrow \infty} \sum_{k=1}^n f(\mu_k) (E_{\mu_k} - E_{\mu_{k-1}})x,$$

where on the right-hand side we are considering the limit of a Riemann sum for any continuous function f and $x \in \mathcal{X}$; see [23, Section 2.3] for a precise definition.

Define $e(\alpha) := \frac{1}{2} \|x^\dagger - x_{\alpha,m,i}^{\delta,h}\|^2$. It follows from the hypothesis that $T_{h,m} x^\dagger = Q_m T x^\dagger = Q_m y$ and

$$\begin{aligned} \frac{de(\alpha)}{d\alpha} &= i \left\langle T_{h,m} x^\dagger - \int_0^\infty \frac{(\mu + \alpha)^i - \alpha^i}{(\mu + \alpha)^i} dF_\mu^{h,m} Q_m y^\delta, \int_0^\infty \frac{\alpha^{i-1}}{(\mu + \alpha)^{i+1}} dF_\mu^{h,m} Q_m y^\delta \right\rangle \\ &= i \left\langle Q_m y - \int_0^\infty \frac{(\mu + \alpha)^i - \alpha^i}{(\mu + \alpha)^i} dF_\mu^{h,m} Q_m y^\delta, \int_0^\infty \frac{\alpha^{i-1}}{(\mu + \alpha)^{i+1}} dF_\mu^{h,m} Q_m y^\delta \right\rangle. \end{aligned}$$

Adding and subtracting $i\alpha^{2i-1} \|(T_{h,m} T_{h,m}^* + \alpha I)^{-\frac{2i-1}{2}} Q_m y^\delta\|^2$, we obtain

$$\begin{aligned} \frac{de(\alpha)}{d\alpha} &= i\alpha^{2i-1} \|(T_{h,m} T_{h,m}^* + \alpha I)^{-\frac{2i-1}{2}} Q_m y^\delta\|^2 \\ &\quad + i \left\langle \int_0^\infty \frac{\alpha^{i-1}}{(\mu + \alpha)^{\frac{1}{2}}} dF_\mu^{h,m} Q_m (y - y^\delta), (T_{h,m} T_{h,m}^* + \alpha I)^{-\frac{2i-1}{2}} Q_m y^\delta \right\rangle, \end{aligned}$$

and collecting $i\|(T_{h,m} T_{h,m}^* + \alpha I)^{-\frac{2i-1}{2}} Q_m y^\delta\| =: K$ from the two terms gives

$$\frac{de(\alpha)}{d\alpha} \geq K \left(\alpha^{2i-1} \|(T_{h,m} T_{h,m}^* + \alpha I)^{-\frac{2i-1}{2}} Q_m y^\delta\| - \left\| \int_0^\infty \frac{\alpha^{i-1}}{(\mu + \alpha)^{\frac{1}{2}}} dF_\mu^{h,m} Q_m (y - y^\delta) \right\| \right).$$

The proposition now follows from

$$\left\| \int_0^\infty \frac{\alpha^{i-1}}{(\mu + \alpha)^{\frac{1}{2}}} dF_\mu^{h,m} Q_m (y - y^\delta) \right\| \leq \alpha^{i-\frac{3}{2}} \delta.$$

□

We now apply this last result to our methods. This requires that we translate our additional hypothesis to establish convergence rates.

Assumption 2. *There hold the equalities*

$$\tilde{\mathcal{R}}_\ell T_n x_n^\dagger = \tilde{T}_n^{(\ell)} x_n^\dagger$$

and

$$\mathcal{R}_\ell T_n x_n^\dagger = T_n^{(\ell)} x_n^\dagger$$

Note that, if the Arnoldi or Golub-Kahan processes do not break down, the operators $V_{n,\ell} V_{n,\ell}^*$ and $V_\ell V_\ell^*$ converges to I_n as ℓ increases. Therefore, the hypotheses of Assumption 2 are close to being satisfied for ℓ large enough. We can estimate the norm of the differences

$$\|(\tilde{\mathcal{R}}_\ell T_n - \tilde{T}_n^{(\ell)}) x_n^\dagger\|_2 = \|\tilde{\mathcal{R}}_\ell T_n (I_n - V_{n,\ell} V_{n,\ell}^*) x_n^\dagger\|_2$$

and

$$\|(\mathcal{R}_\ell T_n - T_n^{(\ell)}) x_n^\dagger\|_2 = \|\mathcal{R}_\ell T_n (I_n - V_\ell V_\ell^*) x_n^\dagger\|_2.$$

However, these quantities might not be monotonic functions of ℓ ; see Example 3 in Section 7.

Proposition 8. *Let Assumption 2 hold and let $\tau = 1$. Set $\tilde{h}_\ell = h_\ell = 0$ and let (9) and (17) be satisfied. Let $\tilde{\alpha}$ and α be the unique solutions of (8) and (16), respectively. Then for all $\alpha' \geq \tilde{\alpha}$ and $\alpha'' \geq \alpha$, we have that $\|x_n^\dagger - \tilde{x}_{\tilde{\alpha},n,i}^{\delta,\ell}\|_2 \leq \|x_n^\dagger - \tilde{x}_{\alpha',n,i}^{\delta,\ell}\|_2$ and $\|x_n^\dagger - x_{\alpha,n,i}^{\delta,\ell}\|_2 \leq \|x_n^\dagger - x_{\alpha'',n,i}^{\delta,\ell}\|_2$.*

Proof. The result follows from Proposition 7 by using Assumption 2. \square

Under Assumption 2, the parameter choice strategy suggested by Proposition 8 results in computed solutions of higher quality than the parameter choice strategy suggested by Proposition 1 and Proposition 4. In fact, since for both equations (8) and (16), the left-hand sides are monotonically increasing, using smaller right-hand sides yields smaller values of the regularization parameter. Moreover, since we now set $\tilde{h}_\ell = 0$ and $h_\ell = 0$, both equations (9) and (17) are usually satisfied for smaller values of ℓ . This means that we can use Krylov spaces of smaller dimension.

Remark 1. *We may use the parameter choice strategy of this section also when Assumption 2 is not satisfied. This is illustrated in the following section.*

7 Computed examples

We apply the iGKT regularization method to solve several ill-posed operator equations. Examples 1, 2 and 3 are image deblurring problems. Example 3 compares the iGKT and iAT methods using the parameter choice strategy of Section 6. Example 4 works with rectangular matrices for which only the iGKT method can be applied. All computations were carried out using MATLAB with about 15 significant decimal digits.

The matrix T_n takes on one of two forms: It either serves as a model for a blurring operator or models a computer tomography operator. The vector $x_n^\dagger \in \mathbb{R}^{n_2}$ is a discretization of the exact solution of (1). Its image $y_n = T_n x_n^\dagger$ is presumed impractical to measure directly. Instead, we know an observable, noise-contaminated vector, $y_n^\delta \in \mathbb{R}^{n_1}$, that is obtained by adding a vector that models noise to y_n . Let the vector $e_n \in \mathbb{R}^{n_1}$ have normally distributed random entries with zero mean. We scale this vector

$$\hat{e}_n := \frac{\xi \|y_n\|_2}{\|e_n\|_2} e_n$$

to ensure a prescribed noise level $\xi > 0$. Then we define

$$y_n^\delta := y_n + \hat{e}_n.$$

Clearly, $\delta := \|y_n^\delta - y_n\|_2 = \xi \|y_n\|_2$. We fix the value ξ for each example such that δ will correspond to $(100 \cdot \xi)\%$ of $\|y\|_2$. To achieve replicability in the numerical examples, we define the “noise” deterministically by setting `seed=11` in the MATLAB function `randn`, which generates normally distributed pseudorandom numbers and which we use to determine the entries of the vector e_n .

The low-rank approximation $T_n^{(\ell)}$ of T_n is computed by applying ℓ steps of the Golub-Kahan process to the matrix T_n with initial vector $v_1 = y_n^\delta / \|y_n^\delta\|_2$. Thus, we first evaluate the Golub-Kahan decomposition (10) and then define the matrix $T_n^{(\ell)}$ by (11). We proceed similarly for the low-rank approximation $\tilde{T}_n^{(\ell)}$ defined by (7). Note that these matrices are not explicitly formed.

Table 2: Example 1 - Relative error in approximate solutions computed by the iGKT method with parameter α determined using (21) for $n = 256$ and $\xi = 1\%$.

ℓ	i	iGKT	
		α	$\ x_n^\dagger - x_{\alpha,n,i}^{\delta,\ell}\ _2 / \ x_n^\dagger\ _2$
80	1	$1.59 \cdot 10^1$	$9.76 \cdot 10^{-1}$
	50	$5.50 \cdot 10^2$	$9.65 \cdot 10^{-1}$
	100	$3.36 \cdot 10^1$	$6.44 \cdot 10^{-1}$
	200	$5.82 \cdot 10^0$	$4.73 \cdot 10^{-1}$
	500	$2.03 \cdot 10^0$	$3.24 \cdot 10^{-1}$
	1000	$1.42 \cdot 10^0$	$2.50 \cdot 10^{-1}$
	2000	$1.19 \cdot 10^0$	$2.17 \cdot 10^{-1}$
160	1	$1.03 \cdot 10^0$	$7.96 \cdot 10^{-1}$
	50	$4.56 \cdot 10^1$	$7.49 \cdot 10^{-1}$
	100	$3.36 \cdot 10^1$	$6.44 \cdot 10^{-1}$
	200	$5.82 \cdot 10^0$	$4.73 \cdot 10^{-1}$
	500	$2.03 \cdot 10^0$	$3.24 \cdot 10^{-1}$
	1000	$1.42 \cdot 10^0$	$2.50 \cdot 10^{-1}$
	2000	$1.19 \cdot 10^0$	$2.17 \cdot 10^{-1}$
240	1	$4.55 \cdot 10^{-1}$	$7.11 \cdot 10^{-1}$
	50	$2.43 \cdot 10^1$	$6.77 \cdot 10^{-1}$
	100	$3.36 \cdot 10^1$	$6.44 \cdot 10^{-1}$
	200	$5.82 \cdot 10^0$	$4.73 \cdot 10^{-1}$
	500	$2.03 \cdot 10^0$	$3.24 \cdot 10^{-1}$
	1000	$1.42 \cdot 10^0$	$2.50 \cdot 10^{-1}$
	2000	$1.19 \cdot 10^0$	$2.17 \cdot 10^{-1}$

We determine the parameter α for Algorithm 4 (iGKT) by solving equation (16) with $C = 1$ and $E = \|x_n^\dagger\|_2$, as suggested by Proposition 4. Inequality (17) holds for all examples of this section. In other words, α is the unique solution of

$$\alpha^{2i+1}(\hat{y}_{\ell+1}^\delta)^*(\Sigma_{\ell+1,\ell}\Sigma_{\ell+1,\ell}^* + \alpha I_{\ell+1})^{-2i-1}\hat{y}_{\ell+1}^\delta = (\|x_n^\dagger\|_2 h_\ell + \delta)^2. \quad (21)$$

We also illustrate the performance of the alternative parameter choice strategy of Section 6. As suggested by Proposition 8, the parameter α for Algorithm 4 (iGKT) is the unique solution of

$$\alpha^{2i+1}(\hat{y}_{\ell+1}^\delta)^*(\Sigma_{\ell+1,\ell}\Sigma_{\ell+1,\ell}^* + \alpha I_{\ell+1})^{-2i-1}\hat{y}_{\ell+1}^\delta = \delta^2. \quad (22)$$

Since we would like to compare the iGKT and iAT methods using the alternative parameter choice strategies suggested by Proposition 8, the parameter $\tilde{\alpha}$ for Algorithm 1 (iAT) is chosen to be the unique solution of

$$\tilde{\alpha}^{2i+1}(\tilde{y}_{\ell+1}^\delta)^*(\tilde{\Sigma}_{\ell+1,\ell}\tilde{\Sigma}_{\ell+1,\ell}^* + \tilde{\alpha} I_{\ell+1})^{-2i-1}\tilde{y}_{\ell+1}^\delta = \delta^2. \quad (23)$$

Example 1. We consider an image deblurring problem and use the function `PRblurspeckle` from the toolbox `IRtools` [24] to determine an $n^2 \times n^2$ matrix T_n that models blurring of an image that is represented by $n \times n$ pixels. This function generates a blurred image with the blur determined by a speckle point spread function that models atmospheric blur.

We set $n = 256$. The true image is represented by the vector $x_n^\dagger \in \mathbb{R}^{n^2}$. This image is shown in Figure 1 (upper left) and the observed image $y_n^\delta \in \mathbb{R}^{n^2}$ (upper right) is obtained by adding white Gaussian noise with $\xi = 1\%$. We test the iGKT method for several values of ℓ and i . Table 2 reports the relative approximation error for the parameter α obtained by solving equations (21). The iGKT method can be seen to perform well.

Table 3 reports the relative approximation errors for the parameter α obtained by solving equation (22). Assumption 2 is not satisfied for this example. Nevertheless, we can try to use this parameter choice rule because it allows a smaller value of ℓ without loss in the quality of the reconstructions.

Figure 1 shows some reconstructed images in the second row.

Example 2. We consider another image deblurring problem and use the function `PRblurshake` from `IRtools` with option `BlurLevel='severe'`. The MATLAB function `rng` is applied with the parameter values `seed=11` and

Table 3: Example 1 - Relative error in approximate solutions computed by the iGKT method with parameter α determined using (22) for $n = 256$ and $\xi = 1\%$.

ℓ	i	iGKT	
		α	$\ x_n^\dagger - x_{\alpha,n,i}^{\delta,\ell}\ _2 / \ x_n^\dagger\ _2$
20	1	$4.17 \cdot 10^{-3}$	$3.75 \cdot 10^{-1}$
	50	$2.58 \cdot 10^{-1}$	$3.54 \cdot 10^{-1}$
	100	$5.17 \cdot 10^{-1}$	$3.54 \cdot 10^{-1}$
	200	$1.04 \cdot 10^0$	$3.54 \cdot 10^{-1}$
	500	$2.03 \cdot 10^0$	$3.42 \cdot 10^{-1}$
	1000	$1.42 \cdot 10^0$	$3.24 \cdot 10^{-1}$
	2000	$1.19 \cdot 10^0$	$3.24 \cdot 10^{-1}$
40	1	$2.23 \cdot 10^{-3}$	$3.09 \cdot 10^{-1}$
	50	$1.19 \cdot 10^{-1}$	$2.84 \cdot 10^{-1}$
	100	$2.37 \cdot 10^{-1}$	$2.83 \cdot 10^{-1}$
	200	$4.75 \cdot 10^{-1}$	$2.83 \cdot 10^{-1}$
	500	$1.19 \cdot 10^0$	$2.83 \cdot 10^{-1}$
	1000	$1.42 \cdot 10^0$	$2.53 \cdot 10^{-1}$
	2000	$1.19 \cdot 10^0$	$2.34 \cdot 10^{-1}$
80	1	$1.59 \cdot 10^{-3}$	$2.84 \cdot 10^{-1}$
	50	$8.32 \cdot 10^{-2}$	$2.59 \cdot 10^{-1}$
	100	$1.67 \cdot 10^{-1}$	$2.59 \cdot 10^{-1}$
	200	$3.33 \cdot 10^{-1}$	$2.59 \cdot 10^{-1}$
	500	$8.34 \cdot 10^{-1}$	$2.59 \cdot 10^{-1}$
	1000	$1.42 \cdot 10^0$	$2.50 \cdot 10^{-1}$
	2000	$1.19 \cdot 10^0$	$2.17 \cdot 10^{-1}$

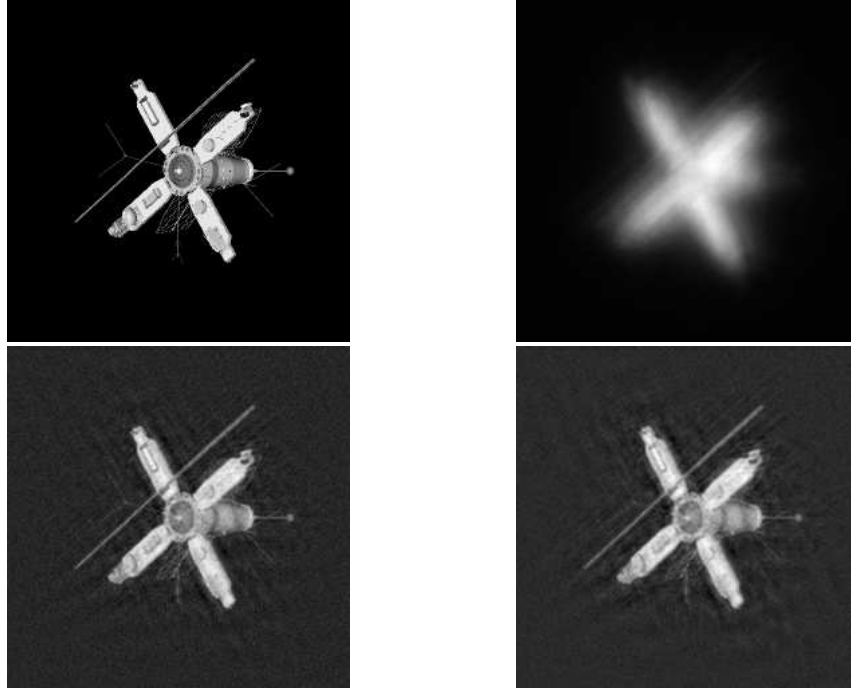


Figure 1: Example 1 - Exact solution x_n^\dagger (upper left) and observed image y_n^δ (upper right). Approximate solutions $x_{\alpha,n,i}^{\delta,\ell}$ computed by the iGKT method with $\ell = 80$ and $i = 2000$ with α determined using (21) (lower left) and $x_{\alpha,n,i}^{\delta,\ell}$ computed by the iGKT method with $\ell = 40$ and $i = 2000$ with α determined using (22) (lower right). Here $n = 256$ and $\xi = 1\%$.

Table 4: Example 2 - Relative error in approximate solutions computed by the iGKT method with parameter α determined using (21) and (22), for $n = 256$ and $\xi = 1\%$.

ℓ	i	iGKT (21)		iGKT (22)	
		α	$\ x_n^\dagger - x_{\alpha,n,i}^{\delta,\ell}\ _2 / \ x_n^\dagger\ _2$	$\tilde{\alpha}$	$\ x_n^\dagger - \tilde{x}_{\tilde{\alpha},n,i}^{\delta,\ell}\ _2 / \ x_n^\dagger\ _2$
30	1	-	-	$7.56 \cdot 10^{-3}$	$1.80 \cdot 10^{-1}$
	50	-	-	$4.04 \cdot 10^{-1}$	$1.64 \cdot 10^{-1}$
	100	-	-	$8.08 \cdot 10^{-1}$	$1.64 \cdot 10^{-1}$
	200	-	-	$1.62 \cdot 10^0$	$1.64 \cdot 10^{-1}$
	500	-	-	$2.02 \cdot 10^0$	$1.45 \cdot 10^{-1}$
60	1	$1.81 \cdot 10^1$	$9.63 \cdot 10^{-1}$	$6.17 \cdot 10^{-3}$	$1.72 \cdot 10^{-1}$
	50	$6.23 \cdot 10^2$	$9.46 \cdot 10^{-1}$	$3.26 \cdot 10^{-1}$	$1.57 \cdot 10^{-1}$
	100	$3.35 \cdot 10^1$	$3.91 \cdot 10^{-1}$	$6.53 \cdot 10^{-1}$	$1.57 \cdot 10^{-1}$
	200	$5.81 \cdot 10^0$	$2.25 \cdot 10^{-1}$	$1.31 \cdot 10^0$	$1.57 \cdot 10^{-1}$
	500	$2.02 \cdot 10^0$	$1.45 \cdot 10^{-1}$	$2.02 \cdot 10^0$	$1.45 \cdot 10^{-1}$
120	1	$1.60 \cdot 10^0$	$7.27 \cdot 10^{-1}$	$5.81 \cdot 10^{-3}$	$1.69 \cdot 10^{-1}$
	50	$6.71 \cdot 10^1$	$6.43 \cdot 10^{-1}$	$3.07 \cdot 10^{-1}$	$1.55 \cdot 10^{-1}$
	100	$3.35 \cdot 10^1$	$3.91 \cdot 10^{-1}$	$6.14 \cdot 10^{-1}$	$1.55 \cdot 10^{-1}$
	200	$5.81 \cdot 10^0$	$2.25 \cdot 10^{-1}$	$1.23 \cdot 10^0$	$1.55 \cdot 10^{-1}$
	500	$2.02 \cdot 10^0$	$1.45 \cdot 10^{-1}$	$2.02 \cdot 10^0$	$1.45 \cdot 10^{-1}$

generator='twister' to determine an $n^2 \times n^2$ blurring matrix T_n and a blurred and noisy image that is represented by $n \times n$ pixels. The blur simulates random camera motion (shaking). The noise is white Gaussian with $\xi = 1\%$.

We set $n = 256$; the true image is represented by the vector $x_n^\dagger \in \mathbb{R}^{n^2}$. This image is shown in Figure 2 (upper left) with the observed image $y_n^\delta \in \mathbb{R}^{n^2}$ (upper right).

Table 4 shows results for the iGKT method with the relative error of the computed approximations corresponding to the parameter α that is determined by solving equation (21) or equation (22) for several values of ℓ and i . Assumption 2 is not satisfied. However, the alternative parameter selection strategy allows smaller values of ℓ .

Reconstructed images for both parameter choice strategies are shown in Figure 2.

Example 3. This example considers the restoration of an image that has been contaminated by motion blur and noise. Thus, we use an $n^2 \times n^2$ psfMatrix T_n that simulates motion blur with $n = 256$. Figure 4 shows the true image represented by $x_n^\dagger \in \mathbb{R}^{n^2}$ (upper left) and the observed blurred and noisy image represented by $y_n^\delta \in \mathbb{R}^{n^2}$ (upper right). The noise is white Gaussian with $\xi = 2\%$.

We compare the iGKT and iAT methods for several values of ℓ and i . The inequalities (9) and (17) are not satisfied. We show results for the alternative parameter choice strategy. Table 5 reports the relative approximation errors for the parameters α and $\tilde{\alpha}$, obtained by solving equations (22) and (23), respectively. Assumption 2 are not satisfied. The iGKT method gives better reconstructions than the iAT method. We also report the average computing times. They show the iAT method to be slightly faster.

Figure 3 displays the relative norm of the difference from Assumption 2 for several values of ℓ . We can see that for the iGKT method this norm decrease rapidly and monotonically, but not for the iAT method. The figure also shows the values of h_ℓ and \tilde{h}_ℓ .

Figure 4 shows some reconstructed images in the second row.

Example 4. This example is concerned with a computerized tomography problem. We use the function PRtomo from IRtools setting $\lfloor n\sqrt{2} \rfloor$ number of rays and 180 uniformly distributed angles from 0 to π , to determine an $180\lfloor n\sqrt{2} \rfloor \times n^2$ matrix T_n . The true image, represented by the vector $x_n^\dagger \in \mathbb{R}^{n^2}$ for $n = 256$, is shown in Figure 5 (upper left). The observed data (the sinogram) $y_n^\delta \in \mathbb{R}^{180\lfloor n\sqrt{2} \rfloor}$ is depicted in Figure 5 (upper right). The noise is $\xi = 1\%$.

Table 6 collects some relative approximation errors for the iGKT method. The parameter α is obtained by solving equation (21) or by solving equation (22) for various values of ℓ and i . Assumption 2 is not satisfied. The alternative parameter selection strategy allows smaller values of ℓ and yields good reconstructions for small values of i .

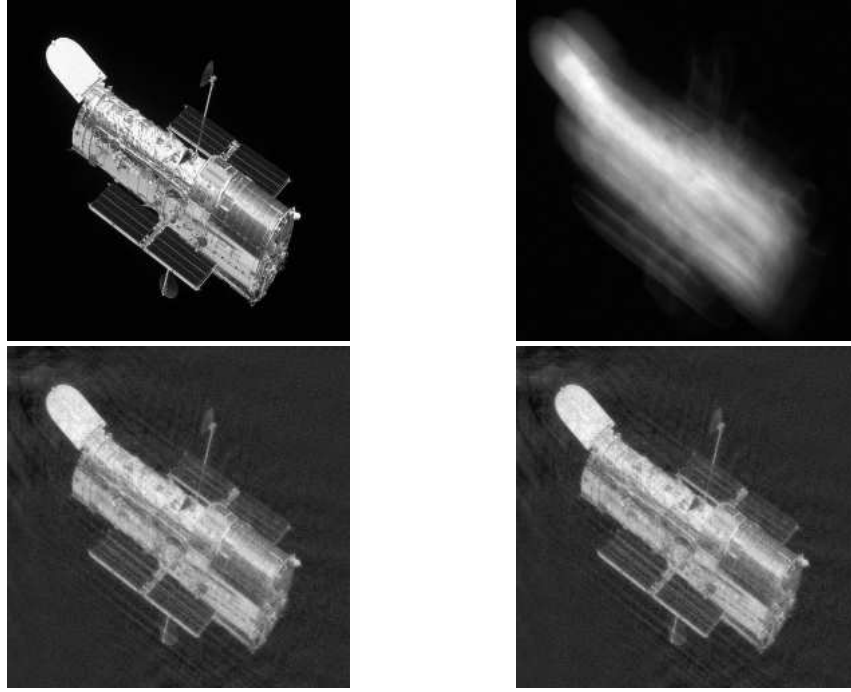


Figure 2: Example 2 - Exact solution x_n^\dagger (Up-Left) and observed image y_n^δ (upper right). Approximate solutions $x_{\alpha,n,i}^{\delta,\ell}$ computed by the iGKT method with $\ell = 60$, $i = 500$, and α determined by solving (21) (lower left) and $x_{\alpha,n,i}^{\delta,\ell}$ computed by the iGKT method with $\ell = 30$, $i = 500$, and α determined using (22) (lower right). Here $n = 256$ and $\xi = 1\%$.

Table 5: Example 3 - Relative error in approximate solutions computed by the iGKT and iAT methods with the parameters α and $\tilde{\alpha}$ determined by using (22) and (23), respectively. Average computing times are reported and $n = 256$ and $\xi = 2\%$.

ℓ	i	iGKT			iAT		
		α	$\ x_n^\dagger - x_{\alpha,n,i}^{\delta,\ell}\ _2 / \ x_n^\dagger\ _2$	time (s)	$\tilde{\alpha}$	$\ x_n^\dagger - \tilde{x}_{\tilde{\alpha},n,i}^{\delta,\ell}\ _2 / \ x_n^\dagger\ _2$	time (s)
10	1	$6.10 \cdot 10^{-2}$	$1.35 \cdot 10^{-1}$	0.26	$6.25 \cdot 10^{-2}$	$1.49 \cdot 10^{-1}$	0.16
	50	$4.83 \cdot 10^0$	$1.24 \cdot 10^{-1}$	0.26	$5.20 \cdot 10^0$	$1.43 \cdot 10^{-1}$	0.16
	100	$9.66 \cdot 10^0$	$1.24 \cdot 10^{-1}$	0.27	$1.04 \cdot 10^1$	$1.43 \cdot 10^{-1}$	0.16
	150	$1.02 \cdot 10^0$	$1.15 \cdot 10^{-1}$	0.27	$1.02 \cdot 10^1$	$1.46 \cdot 10^{-1}$	0.17
	200	$5.72 \cdot 10^0$	$1.02 \cdot 10^{-1}$	0.27	$5.72 \cdot 10^0$	$1.57 \cdot 10^{-1}$	0.17
20	1	$4.96 \cdot 10^{-2}$	$1.26 \cdot 10^{-1}$	0.53	$5.17 \cdot 10^{-2}$	$1.47 \cdot 10^{-1}$	0.32
	50	$3.30 \cdot 10^0$	$1.14 \cdot 10^{-1}$	0.53	$3.69 \cdot 10^0$	$1.44 \cdot 10^{-1}$	0.32
	100	$6.60 \cdot 10^0$	$1.14 \cdot 10^{-1}$	0.54	$7.38 \cdot 10^0$	$1.44 \cdot 10^{-1}$	0.31
	150	$9.90 \cdot 10^0$	$1.14 \cdot 10^{-1}$	0.54	$1.02 \cdot 10^1$	$1.45 \cdot 10^{-1}$	0.32
	200	$5.72 \cdot 10^0$	$1.00 \cdot 10^{-1}$	0.54	$5.72 \cdot 10^0$	$1.58 \cdot 10^{-1}$	0.32
30	1	$4.71 \cdot 10^{-2}$	$1.24 \cdot 10^{-1}$	0.80	$5.12 \cdot 10^{-2}$	$1.46 \cdot 10^{-1}$	0.48
	50	$3.03 \cdot 10^0$	$1.12 \cdot 10^{-1}$	0.80	$3.63 \cdot 10^0$	$1.44 \cdot 10^{-1}$	0.47
	100	$6.06 \cdot 10^0$	$1.12 \cdot 10^{-1}$	0.80	$7.25 \cdot 10^0$	$1.44 \cdot 10^{-1}$	0.48
	150	$9.09 \cdot 10^0$	$1.12 \cdot 10^{-1}$	0.81	$1.02 \cdot 10^0$	$1.45 \cdot 10^{-1}$	0.48
	200	$5.72 \cdot 10^0$	$1.00 \cdot 10^{-1}$	0.80	$5.72 \cdot 10^0$	$1.58 \cdot 10^{-1}$	0.48

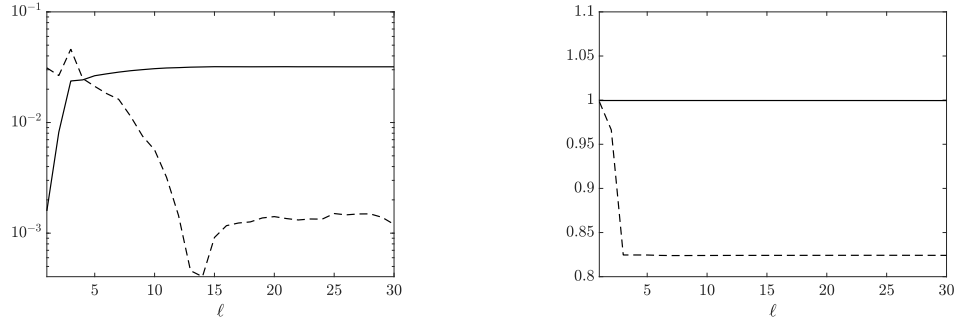


Figure 3: Example 3 - (Left) Values of $\frac{\|(\tilde{\mathcal{R}}_\ell T_n - \tilde{T}_n^{(\ell)})x_n^\dagger\|_2}{\|\mathcal{R}_\ell T_n x_n^\dagger\|_2}$ (continuous line) and $\frac{\|(\mathcal{R}_\ell T_n - T_n^{(\ell)})x_n^\dagger\|_2}{\|\mathcal{R}_\ell T_n x_n^\dagger\|_2}$ (dashed line) in logarithmic scale. (Right) Values of $\frac{\tilde{h}_\ell}{\|T_n\|_2}$ (continuous line) and $\frac{h_\ell}{\|T_n\|_2}$ (dashed line). Here $\ell = 1, \dots, 30$.

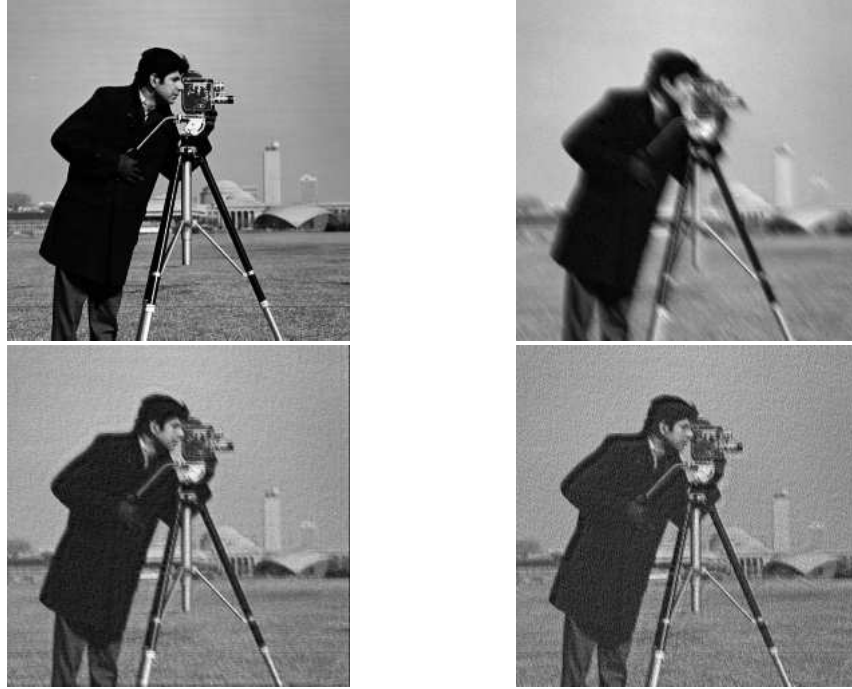


Figure 4: Example 3 - True image x_n^\dagger (upper left) and observed image y_n^δ (upper right). Approximate solutions $x_{\alpha,n,i}^{\delta,\ell}$ computed by the iGKT method with $i = 200$ and α determined using (22) (lower left) and $x_{\alpha,n,i}^{\delta,\ell}$ computed by the iAT method with $i = 100$ and $\tilde{\alpha}$ determined using (23) (lower right) with $\ell = 20$. Here $n = 256$ and $\xi = 2\%$.

Table 6: Example 4 - Relative error in approximate solutions computed by the iGKT method with parameter α determined using (21) and (22), for $n = 256$ and $\xi = 1\%$.

ℓ	i	iGKT (21)		iGKT (22)	
		α	$\ x_n^\dagger - x_{\alpha,n,i}^{\delta,\ell}\ _2 / \ x_n^\dagger\ _2$	$\tilde{\alpha}$	$\ x_n^\dagger - \tilde{x}_{\tilde{\alpha},n,i}^{\delta,\ell}\ _2 / \ x_n^\dagger\ _2$
3	1	-	-	$6.36 \cdot 10^2$	$5.65 \cdot 10^{-1}$
	25	-	-	$3.89 \cdot 10^4$	$5.53 \cdot 10^{-1}$
	50	-	-	$1.03 \cdot 10^3$	$5.47 \cdot 10^{-1}$
	100	-	-	$3.27 \cdot 10^1$	$5.47 \cdot 10^{-1}$
6	1	$1.40 \cdot 10^6$	$9.90 \cdot 10^{-1}$	$2.34 \cdot 10^2$	$3.34 \cdot 10^{-1}$
	25	$9.29 \cdot 10^5$	$8.06 \cdot 10^{-1}$	$1.13 \cdot 10^4$	$3.12 \cdot 10^{-1}$
	50	$1.03 \cdot 10^3$	$2.99 \cdot 10^{-1}$	$1.03 \cdot 10^3$	$2.99 \cdot 10^{-1}$
	100	$3.27 \cdot 10^1$	$2.99 \cdot 10^{-1}$	$3.26 \cdot 10^1$	$2.99 \cdot 10^{-1}$
12	1	$2.59 \cdot 10^5$	$9.52 \cdot 10^{-1}$	$1.47 \cdot 10^2$	$2.22 \cdot 10^{-1}$
	25	$9.29 \cdot 10^5$	$8.06 \cdot 10^{-1}$	$5.76 \cdot 10^3$	$1.96 \cdot 10^{-1}$
	50	$1.03 \cdot 10^3$	$1.78 \cdot 10^{-1}$	$1.03 \cdot 10^3$	$1.78 \cdot 10^{-1}$
	100	$3.27 \cdot 10^1$	$1.78 \cdot 10^{-1}$	$3.27 \cdot 10^1$	$1.78 \cdot 10^{-1}$

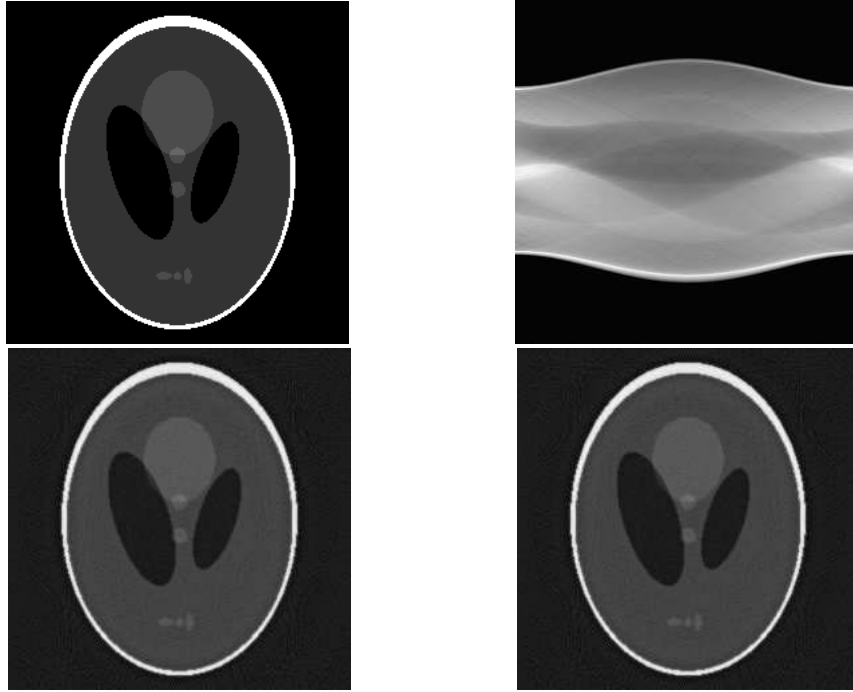


Figure 5: Example 4 - Exact solution x_n^\dagger (Up-Left) and observed data (sinogram) y_n^δ (upper right). Approximate solutions $x_{\alpha,n,i}^{\delta,\ell}$ computed by the iGKT method with α determined by (21) (lower left) and $x_{\alpha,n,i}^{\delta,\ell}$ computed by the iGKT method with α determined by (22) (lower right) with $\ell = 12$ and $i = 50$. Here $n = 256$ and $\xi = 1\%$.

Two reconstructions are shown in the second row of Figure 5.

8 Conclusions

The paper presents a convergence analysis for iterated Tikhonov regularization based on partial Golub-Kahan bidiagonalization. Two approaches for choosing the regularization parameter are discussed.

Acknowledgments

D. Bianchi is supported by the Startup Fund of Sun Yat-sen University. M. Donatelli is partially supported by MIUR - PRIN 2022 N.2022ANC8HL and GNCS-INdAM Project CUP_E53C24001950001.

References

- [1] P. Díaz de Alba, L. Fermo, C. van der Mee, and G. Rodriguez. “Recovering the electrical conductivity of the soil via a linear integral model”. In: *Journal of Computational and Applied Mathematics* 352 (2019), pp. 132–145.
- [2] M. Alkilayh and L. Reichel. “Some numerical aspects of Arnoldi-Tikhonov regularization”. In: *Applied Numerical Mathematics* 185 (2023), pp. 503–515.
- [3] A. Alqahtani, R. Ramlau, and L. Reichel. “Error estimates for Golub-Kahan bidiagonalization with Tikhonov regularization for ill-posed operator equations”. In: *Inverse Problems* (2023), p. 025002.
- [4] A. H. Bentbib, M. El Guide, K. Jbilou, E. Onunwor, and L. Reichel. “Solution methods for linear discrete ill-posed problems for color image restoration”. In: *BIT Numerical Mathematics* 58 (2018), pp. 555–578.
- [5] D. Bianchi, A. Buccini, M. Donatelli, and S. Serra-Capizzano. “Iterated fractional Tikhonov regularization”. In: *Inverse Problems* 31.5 (2015), p. 055005.
- [6] D. Bianchi, M. Donatelli, D. Furchí, and L. Reichel. “Convergence analysis and parameter estimation for the iterated Arnoldi-Tikhonov method”. In: *Numerische Mathematik* 157 (2025), pp. 749–779.
- [7] Å. Björck. “A bidiagonalization algorithm for solving large and sparse ill-posed systems of linear equations”. In: *BIT Numerical Mathematics* 18 (1988), pp. 659–670.
- [8] Å. Björck. *Numerical Methods for Least Squares Problem*. SIAM, Philadelphia, 202A.
- [9] Å. Björck. *Numerical Methods in Matrix Computations*. Springer, New York, 2014.
- [10] C. de Boor. *A Practical Guide to Splines*. Springer, 1978.
- [11] A. Buccini, M. Donatelli, and L. Reichel. “Iterated Tikhonov regularization with a general penalty term”. In: *Numerical Linear Algebra with Applications* 24.4 (2017), e2089.
- [12] A. Buccini, L. Onisk, and L. Reichel. “An Arnoldi-based preconditioner for iterated Tikhonov regularization”. In: *Numerical Algorithms* 92.1 (2023), pp. 223–245.
- [13] A. Buccini, M. Pasha, and L. Reichel. “Generalized singular value decomposition with iterated Tikhonov regularization”. In: *Journal of Computational and Applied Mathematics* 373 (2020), p. 112276.
- [14] D. Calvetti, B. Lewis, and L. Reichel. “Restoration of images with spatially variant blur by the GMRES method”. In: *Advanced Signal Processing Algorithms, Architectures, and Implementations X, ed. F. T. Luk, Proceedings of the Society of Photo-Optical Instrumentation Engineers (SPIE)*. Vol. 4116. 2000, pp. 364–374.
- [15] D. Calvetti, S. Morigi, L. Reichel, and F. Sgallari. “Tikhonov regularization and the L-curve for large discrete ill-posed problems”. In: *Journal of Computational and Applied Mathematics* 123.1-2 (2000), pp. 423–446.
- [16] D. Calvetti and L. Reichel. “Tikhonov regularization of large linear problems”. In: *BIT Numerical Mathematics* 43 (2003), pp. 263–283.
- [17] M. Donatelli. “On nondecreasing sequences of regularization parameters for nonstationary iterated Tikhonov”. In: *Numerical Algorithms* 60 (2012), pp. 651–668.
- [18] M. Donatelli, D. Martin, and L. Reichel. “Arnoldi methods for image deblurring with anti-reflective boundary conditions”. In: *Applied Mathematics and Computation* 253 (2015), pp. 135–150.
- [19] L. Eldén. “A weighted pseudoinverse, generalized singular values and constraint least squares problems”. In: *BIT Numerical Mathematics* 2 (1982), pp. 487–502.
- [20] L. Eldén. “Algorithms for the computation of functionals defined on the solution of a discrete ill-posed problem”. In: *BIT Numerical Mathematics* 30 (1990), pp. 466–483.
- [21] L. Eldén. “Algorithms for the regularization of ill-conditioned least squares problems”. In: *BIT Numerical Mathematics* 17 (1977), pp. 134–145.
- [22] L. Eldén, P. C. Hansen, and M. Rojas. “Minimization of linear functionals defined on solutions of large-scale discrete ill-posed problems”. In: *BIT Numerical Mathematics* (2005), pp. 329–340.
- [23] H. W. Engl, M. Hanke, and A. Neubauer. *Regularization of Inverse Problems*. Kluwer, Dordrecht, 1996.
- [24] S. Gazzola, P. C. Hansen, and J. G. Nagy. “IR Tools: a MATLAB package of iterative regularization methods and large-scale test problems”. In: *Numerical Algorithms* 81 (2019), pp. 773–811.
- [25] S. Gazzola, P. Novati, and M. R. Russo. “On Krylov projection methods and Tikhonov regularization”. In: *Electronic Transactions on Numerical Analysis* 44 (2015), pp. 83–123.

- [26] G. H. Golub and C. F. Van Loan. *Matrix Computations*, 4th ed. Johns Hopkins University Press, Baltimore, 2013.
- [27] R. W. Goodman. *Discrete Fourier and Wavelet Transforms: An Introduction through Linear Algebra with Applications to Signal Processing*. World Scientific Publishing Company, London, 2016.
- [28] L. Greengard and V. Rokhlin. “A new version of the fast multipole method for the Laplace equation in three dimensions”. In: *Acta Numerica* 6 (1997), pp. 229–269.
- [29] M. Hanke and C. W. Groetsch. “Nonstationary iterated Tikhonov regularization”. In: *Journal of Optimization Theory and Applications* 98 (1998), pp. 37–53.
- [30] B. Lewis and L. Reichel. “Arnoldi-Tikhonov regularization methods”. In: *Journal of Computational and Applied Mathematics* 226 (2009), pp. 92–102.
- [31] F. Natterer. “Regularization of ill-posed problems by projection methods”. In: *Numerische Mathematik* 28 (1977), pp. 329–341.
- [32] F. Natterer. *The Mathematics of Computerized Tomography*. SIAM, Philadelphia, 2001.
- [33] A. Neubauer. “An a posteriori parameter choice for Tikhonov regularization in the presence of modeling error”. In: *Applied Numerical Mathematics* 4 (1988), pp. 507–519.
- [34] S. Raffetseder, R. Ramlau, and M. Yudyski. “Optimal mirror deformation for multi-conjugate adaptive optics systems”. In: *Inverse Problems* 32 (2016), p. 025009.
- [35] R. Ramlau and L. Reichel. “Error estimates for Arnoldi-Tikhonov regularization for ill-posed operator equations”. In: *Inverse Problems* 35 (2019), p. 055002.
- [36] R. Ramlau and M. Rosensteiner. “An efficient solution to the atmospheric turbulence tomography problem using Kaczmarz iteration”. In: *Inverse Problems* 28 (2012), p. 095004.
- [37] Y. Saad. *Iterative Methods for Sparse Linear Systems*. 2nd. SIAM, Philadelphia, 2003.